ISSN (Print) 1226-1750
ISSN (Online) 2233-6656
Journal of Magnetics 17(4), 233-241 (2012) http://dx.doi.org/10.4283/JMAG.2012.17.4.233

Time Resolved Effect of Heat Dispersion on Magnetic Stability in Ferromagnetic Ising Thin-Films: Monte Carlo Simulation

W. Laosiritaworn[1] and Y. Laosiritaworn[2,3]*

[1]*Department of Industrial Engineering, Faculty of Engineering, Chiang Mai University, Chiang Mai 50200, Thailand*
[2]*Department of Physics and Materials Science, Faculty of Science, Chiang Mai University, Chiang Mai 50200, Thailand*
[3]*Thailand Center of Excellence in Physics, Commission on Higher Education, Ministry of Education, Bangkok 10400, Thailand*

(Received 9 July 2012, Received in final form 20 November 2012, Accepted 20 November 2012)

In this work, Monte Carlo simulation was used to investigate the magnetization properties of thin ferromagnetic films under a perturbation from a supplied heat pulse on one surface of the films. The finite difference method was used to extract the local temperature of each layer of the films as a function of time for various heat source power and heating period. Then, with the variation of the films temperature, Metropolis method was used to update the magnetic moment in magnetic grain, under the Ising framework and using the FePt parameters. With the extracted magnetization profiles, the relationship between magnetization relaxation in accordance with relevant heat parameters and films thickness was reported and discussed, with a purpose to form a database for future use.

Keywords : magnetization processes, Monte Carlo methods, thermomagnetic, thin-films

1. Introduction

The ferromagnetic multilayer (thin films) have been a subject of intensive interests due to a broad range of applications especially in magnetic recording applications [1]. In terms of fundamental interest, the physical mechanisms involved in these reduced structure systems are quite different from bulk properties has become a topic of frequent investigating issues. For instance, the magnetic properties in thin-films and their associated morphologies are thoroughly different from the bulk [2]. Therefore, one may control the films' thicknesses [3] or films' surface-morphology [4] to obtain the desired magnetic properties in designing applications. On the other hand, in terms of technological interest, how to enhance the magnetic recording application, so the recording capacity is always matching with the customer's need, is nowadays a big issue. Therefore, very high coercive field materials were developed to surpass the 'superparamagnetic effect' [5]. However, this leads to another problem as the write field from the writing head may not be large enough to overcome the coercivity and hence the magnetic data cannot be written. One way out of this problem is to use the heat assisted technique where the thermal energy (e.g. from laser) is applied onto the target to reduce the magnetic stability before writing operation takes place. Nevertheless, due to the materials complexity arisen from the films reduced structure and magnetocaloric effect [6], the detailed understanding in such heat assisted topic is still far from completeness. This severely slows down the technological development in hard disk drive industry. Consequently, it is the objective of this study to investigate the magnetic properties in thin ferromagnetic films under the temperature variation inside the ferromagnetic films due to the heat applied on the topmost surface. In this work, Monte Carlo simulation and spin Hamiltonian [7] were used to investigate the magnetization property in relating to the films thickness, the heat source power, and heat applying duration as a function of time. Since this work aims to model the effect of thermal perturbation in highly anisotropic materials, the $L1_0$-FePt (which is based on crystalline ordering of face-centered tetragonal structure) was chosen as at this phase it has very large magneto-crystalline anisotropy (i.e. 7×10^7 erg/cm^3 [8] or 6.6×10^7 to 10^8 erg/cm^3 [9]). Further, the $L1_0$-FePt particles are thermally stable at room temperature even at nanometer dimensions such as at 4 nm [10], although the recent smallest reported size is 2.2 nm with coercivity of 24 kOe and somewhat

*Corresponding author: Tel: +66-53-94-3367
Fax: +66-53-94-3445, e-mail: yongyut_laosiritaworn@yahoo.com

relatively large spacing between grains of 4.2 nm. In addition, its critical temperature is quite high (about 750 K at bulk form [9]) but not too high for the current available laser technology using in heat assisted recording application [11]. As a result, the parameters of $L1_0$-FePt were used in the simulation.

Note that there has been an intense interest on the study of FePt materials as it could be a promising magnetic recording candidate in heat assisted magnetic recording (HAMR) application. One of the pioneer works on FePt/FePd materials from theoretical side is to use first-principles theory to computationally calculate temperature dependent magnetic anisotropy K and magnetization m via the local moment theory [12]. The study suggested that the $L1_0$-ordered FePt/FePd has the uniaxial anisotropy K being associated to magnetic easy axis perpendicular to the Fe layers and proportional to m^2, in agreement with previous studies (e.g. [13]). In addition, apart from quantum mechanical treatment, there has been considerable effort in studying the FePt properties via micromagnetic simulation under the framework of Landau-Liftshitz-Gilbert (LLG) equation [14]-[17] or Landau-Lifshitz-Bloch (LLB) equation [18]. However, both LLG or LLB reduce all the spins into a single magnetization parameter interacting with appropriate effective field and extract relevant properties from solving the differential equations. As a result, random fluctuation effect on particular spins are discarded, which may cause some problems in the same way as the mean-field analysis overestimates critical temperature of classical spin Hamiltonian problems. Therefore, with the strong anisotropy in the direction perpendicular to the film surface and by taking random thermal effect into account, the Ising spins and Monte Carlo simulation were used in this work.

2. Heat Conduction

In this work, the ferromagnetic material in thin-films structure was considered. Each layer of the films was assumed to be consisting of small magnetic grains where a single magnetic spin was used to represent the grain magnetization. Then, an amount of heat (in a pulse-like) was applied on the topmost layer of the films for duration of time t_0. As a result, the temperature at the surface was then raised which can be calculated from

$$P\delta t = C\delta T, \tag{1}$$

or

$$\delta T = \frac{P\delta t}{C} = \frac{P\delta t}{Vc_V}, \tag{2}$$

where P is the heat source power, δt is the duration of the heat applying, C is the heat capacity, V is the volume, c_V is the volume specific heat and δT is a small change in temperature.

Then with the rise in temperature at the surface layer, the difference in temperature leads to heat transferring from higher temperature to lower temperature layers. In such the situation, all layers below the surface absorbs transferred heat and have their temperatures raised. The finite different method was used to evaluate the time-dependent temperature-variation due to the heat transferring from high temperature to low temperature regions. This can be done by considering the amount of heat coming in and going out a specific region located at the coordinate (x, y, z) with a volume $\delta V = \delta x\delta y\delta z$. Then, the amount of heat left in the volume gives rise to temperature increasing i.e.

$$\sum_{x_i=\{x,y,z\}} (q_{x_i} - q_{x_i+\delta x_i}) = \rho c\,\delta V \frac{\partial T}{\partial t}, \tag{3}$$

where q_{x_i} is the amount of heat supplied into the volume at the position x_i, $-q_{x_i+\delta x_i}$ is the amount of heat leaving the volume, c is the mass specific heat and ρ is the volume density. Next, with the Fourier's heat conduction i.e.

$$q_{x_i} = -k_{x_i}\delta x_{i+1}\delta x_{i+2}\frac{\partial T}{\partial x}, \tag{4}$$

and its Taylor's series expansion around x i.e.

$$q_{x_i+\delta x_i} = q_{x_i} + \frac{\partial q_{x_i}}{\partial x_i}\delta x_i + \cdots, \tag{5}$$

it is possible to write, under the assumption that $(\delta x_i)^n \to 0$ for $n \geq 2$, that

$$q_{x_i+\delta x_i} - q_{x_i} \approx \frac{\partial}{\partial x_i}\left(k_{x_i}\delta x_{i+1}\delta x_{i+2}\frac{\partial T}{\partial x_i}\right)\delta x_i. \tag{6}$$

Note that if x_i refers to the x direction, x_{i+1} and x_{i+2} become y and z directions respectively. After that, if $k_{x_{\{i\}}} = k$ and $\delta x_{\{i\}} = \delta x$, Eq. (3) turns to

$$\sum_{x_i=\{x,y,z\}} (q_{x_i} - q_{x_i+\delta x_i}) = \sum_{x_i=\{x,y,z\}} \frac{\partial^2 T}{\partial x_i^2} = \frac{\rho c}{k}\frac{\partial T}{\partial t}, \tag{7}$$

or

$$\frac{\partial^2 T}{\partial x^2} + \frac{\partial^2 T}{\partial y^2} + \frac{\partial^2 T}{\partial z^2} = \frac{\rho c}{k}\frac{\partial T}{\partial t}. \tag{8}$$

Further, if δx is small, it is possible to write the spatial temperature derivatives at time $t = n\delta t$ as

$$\frac{\partial^2 T^n}{\partial x^2} = \frac{T^n_{x+\delta x,y,z} - 2T^n_{x,y,z} + T^n_{x-\delta x,y,z}}{(\delta x)^2}, \tag{9}$$

and so do $\partial^2 T^n/\partial y^2$ and $\partial^2 T^n/\partial z^2$. For the time deriva-

tive, it can be assumed that

$$\frac{\partial T}{\partial t} = \frac{T_{x,y,z}^{n+1} - T_{x,y,z}^{n}}{\partial t}, \tag{10}$$

which yield good accuracy as long as δt is small enough. Therefore, by substituting these equations into Eq. (8), the temperature at a time $t = (n+1)\delta t$ is given by

$$T_{x,y,z}^{n+1} = T_{x,y,z}^{n} + \frac{k\delta t}{(\delta x)^2 \rho c}\begin{pmatrix} T_{x+\delta x,y,z}^{n} + T_{x-\delta x,y,z}^{n} + \\ T_{x,y+\delta y,z}^{n} + T_{x,y-\delta y,z}^{n} + \\ T_{x,y,z+\delta z}^{n} + T_{x,y,z-\delta z}^{n} - 6T_{x,y,z}^{n} \end{pmatrix}. \tag{11}$$

However, with the finite difference method, the amount of time step has to satisfy $\delta t \le (\delta x)^2 \rho c/k$ 1/6 for $T_{x,y,z}^{n+1}$ in Eq. (11) to converge. In this work, δx was considered be the diameter of a magnetic grain that small enough to exist only a single domain. Then by taking $L1_0$-FePt parameters as an application, the relevant parameters are $\rho c = C/V = c_V \approx 3.16 \times 10^6$ J/K-m^3 [19] and the smallest grain-size, while preserving the $L1_0$ structure, as $\delta x \approx 4$ nm [20]. However, the heat conductivity k tends to very much dependent on the system structure, especially at the nano-ranged scale, making it to be different from its bulk value. These could be due to the enhanced surface to volume ratio where air-gap between grains tends to have negative influences on heat transferring. Therefore, to have the extracted temperature results in an appropriate and reasonable range, $k \approx 1.5$ W/m-K was used in this study. After that, based on these parameters, it is found that $\delta t \le 0.56 \times 10^{-11}$ s. Therefore, much smaller time step $\delta t = 10^{-13}$ s was used for the benefit of accurateness in this work.

3. Monte Carlo Simulation

In this work, the system energy, in the absence of external magnetic field, was considered to take spin Hamiltonian form i.e.

$$H = -\sum_{\langle i,j \rangle} J_{ij} \vec{s}_i \cdot \vec{s}_j, \tag{12}$$

where $\vec{s}_i$ is the magnetic spin representing overall magnetic dipole moment at grain i^{th}, $J_{ij} = J$ is the exchange interaction between spins, and the notation $<ij>$ refers to that only interaction between nearest neighboring grains was considered in the sum.

In general, the heat assisted technology is used due to that the considered magnetic recording media is equipped with very high anisotropy, such as FePt have very large uniaxial anisotropy as $K_u = 6.6 \times 10^7$ to 10^8 erg/cm^3 [9]. At a point that the write field is not strong enough to erase or write digital data (or switch the magnetization direction), thermal energy is then needed to supply onto the media to reduce the coercive field and the magnetic stability. As a result, the media magnetization can be switched with an appropriate intermediate write field. Consequently, to represent this high anisotropy material, the infinite anisotropy Ising spin was considered in the Hamiltonian Eq. (12). In the Ising model, the spins take only values $\vec{s}_i = \pm 1\hat{z}$ (or $s_i = \pm 1$) where $\hat{z}$ is normal to the film. In addition, $J = 1$ was set as the energy unit. Consequently, this defines the energy in the unit of J and the temperature in a unit of J/k_B. Note that the spin s_i is dimensionless as its real magnetic moment unit is absorbed into J. Next, by considering that the heat is from laser source with a spot size of 550 nm [21], the recording media is of a few of 10-nm thickness, and the grain size is about 4 nm [20], the simulated films was chosen to consist of $N = L \times L \times l$ spins (grains), where $L^2 = 140^2$ is the films size and l, ranging from 2 layers to 9 layers, is the films thickness.

In performing the Monte Carlo simulation, all spins were initialized (fully magnetized) to the $+\hat{z}$ direction. Free boundary condition was taken on the surface layers (above the topmost and below the bottommost), but periodic boundary condition was used along the in-plane (xy) directions. After that, an amount of heat, from a heat source with power P, was applied to the topmost layer of the films for the duration of time t_0, and then switched off afterward. Consequently, the temperature was raised according to Eq. (2), and spread out to lower layers, where the temperature at time $t = (n+1)\delta t$ can be calculated using Eq. (11). However, whenever the heat applying is turned off, the temperature of the topmost layer drops due to heat convection to the room temperature environment and the heat conduction to layers below. In addition, the periodic boundary conditions along the xy directions also apply for the temperature of the grains located at the boundaries. Furthermore, the bottommost layer was attached to a heat-sink layer, having a fixed temperature equal to room temperature.

In updating the spin configurations, a random spin was chosen and flipped to its opposite direction, i.e. from s_i to $-s_i$, with the Metropolis probability

$$prob = \exp\left(\frac{-\Delta E_i}{k_B T}\right), \tag{13}$$

where ΔE_i is the energy difference due to the update (flip) on the spin s_i. The spin flipping is accepted if a uniform random number r in the range [0,1) is smaller than the Metropolis probability i.e. $r \le prob$. The general time-unit of Monte Carlo simulation is 1 mcs (Monte Carlo step per site) which equals to N trial flips (either successful or

unsuccessful flips). Further details of the Monte Carlo procedures performing on Ising thin-films can be found elsewhere [23]-[25].

Based on the Stoner and Wohlfarth's picture, the Arrhenius thermal activation leads to an inverse of the relaxation time constant for a ferromagnetic particle in switching its stable directions between two equivalent energy wells as [26]-[27]

$$\tau^{-1}(T) = f_0 \exp\left(-\frac{E_B}{k_B T}\right), \tag{14}$$

where f_0 is an attempted switching frequency estimated to be in the order 10^9 to 10^{12} Hz. By taking the 10^{12} Hz threshold and the limit that each individual magnetic grain can switch freely (i.e. $k_B T \to \infty$ or the paramagnetic state), it is appropriate to scale 1 mcs with the 10^{-12} *s*. As in the heat conduction process, the time step *dt* required for evaluating finite difference is 10^{-13} s. Therefore, in this work, local temperature of each magnetic spin will be updated every $10^{-13}/10^{-12}$ N^{-1} or 0.1 mcs. Next, at the end of each temperature update the (normalized) magnetization per spin for the time t was calculated from

$$m(t) = \frac{1}{N}\sum_i s_i . \tag{15}$$

Then, with varying the power of the heat source P and heat applying duration t_0, the system temperature, the normalized magnetization and its stability profiles (in time domain) were investigated.

4. Computational Setup

In this work, the environment temperature was assumed to be the room temperature i.e. $T_{rm} = 300$ K. As the 3 dimensional Ising model have a critical point about 4.511 J/k_B [28] and the critical temperature of the FePt is T_C = 750 K , it is possible to estimate $T_{rm} = 4.511 \times 300/750 \approx 1.80$ in J/k_B unit. Note that in reduced films structure, the critical temperature of the films system may not as high as that of the bulk due to the surface effect even the magnitude of the exchange interaction is preserved [2].

In the considered films structure, the first layer (or layer 1) was the topmost layer where the heat was applied onto, and the last layer (or layer l) was the bottommost layer. Temperature below the bottommost layer was fixed at T_{rm} during the simulation. However, whenever an amount of heat ($P\delta t$) is applied onto the first layer, the temperature in the first layer rises according to Eq. (2), and dissipates via Eq. (11). Since each layer has a total volume of $140 \times 140 \times 4^3$ $nm^3 = 1.2544 \times 10^6$ nm^3 and $\rho c = c_V \approx 3.15 \times 10^6$ J/K-m^3 [19], the increase in temperature is about $0.2531 \times 10^2 P$ K or $0.1522P$ J/k_B every $\delta t = 10^{-13}$ s (or 0.1 mcs) during the heat applying. In this work, the power of the applied heat source was ranged from at 4 to 20 mW with the duration of heat supplying ranging from t_0 = 0 to 2.0 ns (or t_0 = 0 to 2,000 mcs). Then, after the heat source was switched off, the films system was left for cooling until the total observation time was 3.0 ns (or 3,000 mcs).

During the heating and cooling processes, temperatures of each layer were evaluated as a function of time via Eq. (2) for $t < t_0$ (on the topmost layer) and the finite difference technique via Eq. (11) with $k\delta t/(\delta x)^2 \rho c = 2.97 \times 10^{-3}$ for all layers.

5. Results and Discussion

From the Monte Carlo simulation, the temperature and magnetization profiles were obtained. For instance, Fig. 1a shows the surface temperature (topmost layer) of the 3 layered films due to a heat pulse applying onto the surface layer of the films. In the figure, the presented results are from heat source with power P = 8 mW and 12 mW, where each curve is from different duration of heating time t_0 ranging from t_0 = 0.2 ns to 1.0 ns (for 8 mW) and from t_0 = 1.2 to 2.0 ns (for 12 mW). Considering the 8 mW case, it is found that the temperature of the films rises during the heat applying (i.e. up to t_0) and drops when the heat source is switched off. Numbers in parenthesis indicate duration of heating time and maximum surface temperature i.e. (t_0, $T_{\max}$). As can be seen, with the longer time than t_0, the films system takes longer time to decline in approaching the room temperature level. On the other hand, by increasing the source power P, i.e. from P = 8 mW to 12 mW, the temperature rising rate at the beginning increases due to larger amount of heat is applied onto the system at the same period of time. After that, when temperature is very high, the temperature rising rate starts to drop and ceases to zero implying that the system is now in its steady state in accordance with Fourier's law of heat conduction.

On the other hand, Fig. 1b shows the results the 5 layered films. As can be seen, $T_{\max}$ in Fig. 1b is higher than those in Fig. 1a. This is as in 5 layered films, the films are thicker and there are more magnetic grains in the system. As a result, the 5 layered films can absorb more heat and consequently it transfers less heat to the heat-sink layer in the same period of time compared to that of the 3 layered films. Therefore, it will take longer time for the thicker films to arrive the steady state condition which brings about larger maximum temperature $T_{\max}$ on the surface layer.

On considering the temperature effect on the system magnetization, Fig. 2 shows the normalized magnetization

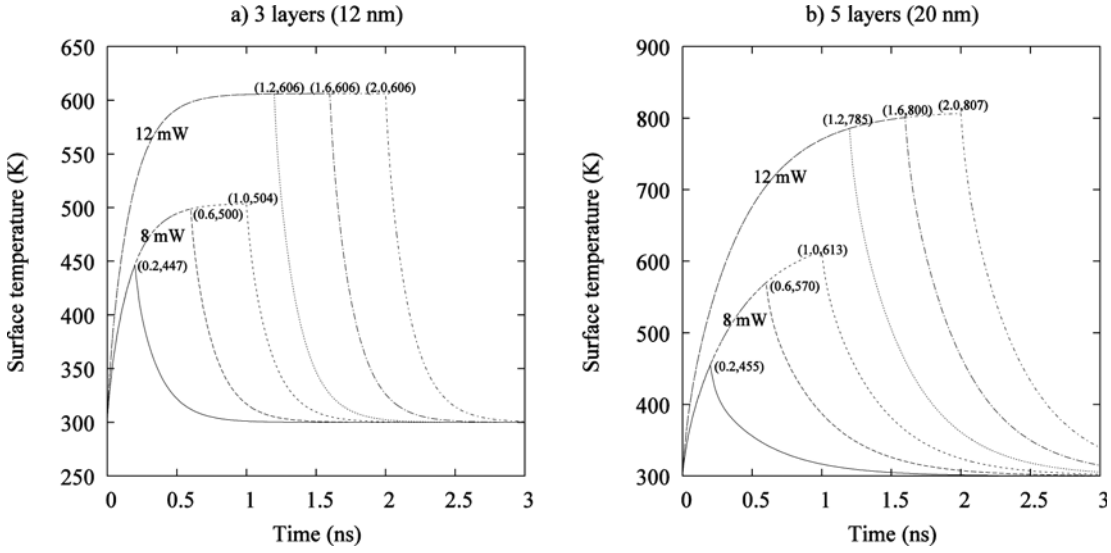

Fig. 1. The topmost surface temperature of films with (a) 3 layers and (b) 5 layers as a function of observed time. The figures show results using heat sources with power P = 8 mW and 12 mW where each curve is from different duration of heating time t_0 ranging from 0.2 to 1.0 ns (for 8 mW) and 1.2 to 2.0 ns (for 12 mW). The total observed time is 3.0 ns. Numbers in parenthesis are duration of heating time and maximum surface temperature i.e. (t_0, T_{max}).

m as a function of observed time of films with 3 layers and 5 layers respectively. The considered power source are P = 12 mW and 20 mW and the duration of heating time are t_0 = 0.2, 0.6 and 1.0 ns (for 12 mW) and t_0 = 1.2, 1.6 and 2.0 ns (for 20 mW). As can be seen, e.g. considering Fig. 2a, the normalized magnetization m reduces in time when the heat source is switched on (up to t_0), and later changes to increase when the heat source is switched off. Being obvious, with larger heat applied duration t_0, the magnetization m has lower minimum value (m_{min}). This is as, from Fig. 1, the larger t_0 brings about larger temperature T on the surface layer. Therefore, with the higher temperature, this larger level of thermal fluctuation reduces the ferromagnetic order and lessens the magnetization value. However, when the heat source is switched off (at $t > t_0$), the system temperature drops to room temperature

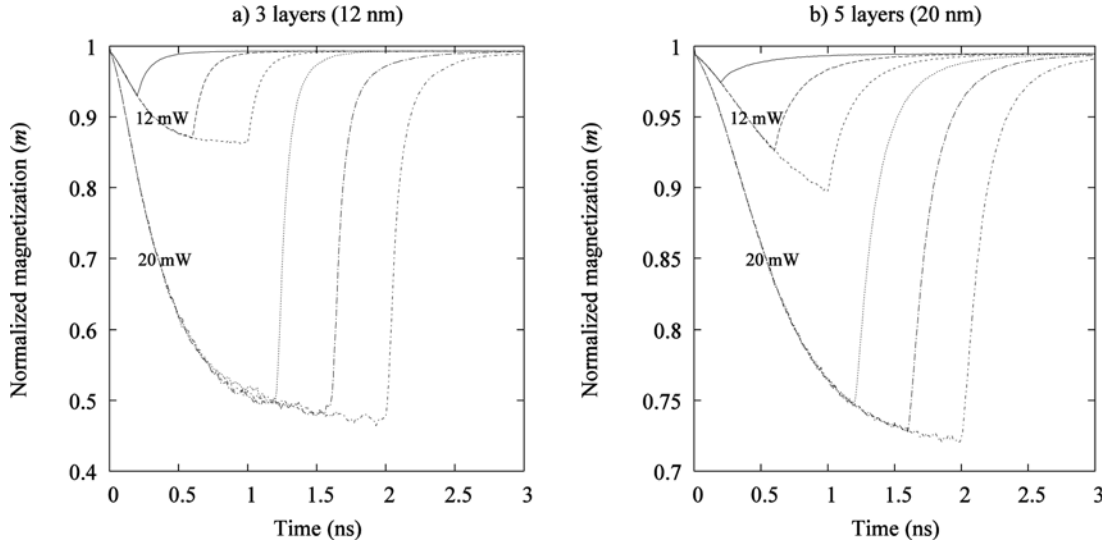

Fig. 2. The normalized magnetization m as a function of observed time of films with (a) 3 layers and (b) 5 layers. The results are for heat sources with power P = 12 and 20 mW where the duration of heating time t_0 ranges from 0.2 to 1.0 ns (for 12 mW) and 1.2 to 2.0 ns (for 20 mW). The total observed time is 3.0 ns. The time where minimum normalized magnetization occurs matches with t_0 (not shown).

so the ferromagnetic order grows and enhances the magnetization to its appropriate value at room temperature. Alternatively, Fig. 2b shows similar results but for 5 layered films. It is found that the minimum normalized magnetization at t_0 ($m_{\min}$) is larger than those in Fig. 2a (the 3 layered films) even at the same heating condition. This is expected as the thicker films have more number of magnetic grains to absorb the heat, so the average films temperature (not the surface temperature) of the 5 layered films is smaller. Therefore, $m_{\min}$ is larger than those of the 3 layered films. This implies that the thicker films require more heat in reducing ferromagnetic stability to a specific desired value.

Note that according to Stoner-Wohlfarth theory, the anisotropy field H_k of a single-domain magnetic-particle is identical to the switching field H_c. Further, the temperature dependence of the anisotropy field takes the form $H_k = 2K(T)/M_s(T)$, where $K(T)$ is temperature dependent magneto-crystalline anisotropy, and M_s is the temperature dependent saturation magnetization. Relative to M_s the anisotropy K drops faster with temperature, as for the $Fe_{55}Pt_{45}$ film it is found that $K(T)/K(0) = (M_s(T)/M_s(0))^2$ [29]. Therefore, H_k scales with M_s and the reduction in the magnetization linearly influence the reduction in anisotropy field (e.g. $Fe_{55}Pt_{45}$ films [29]) and hence the writing field. Therefore, if the writing field is about 10 kOe and the room temperature anisotropy field is about 82 kOe [29], the reduction ratio of (82-10)/82 ≈ 88% in anisotropy field and the magnetization is considered significant in the writing process. Using this proposed relation, one can trivially re-calculate the significant amount of magnetization reduction in the writing process if this writing field is changed.

Further, it is also of interest to discuss the temperatures obtained from the simulation whether or not they are in line with those in real application. In heat-assisted magnetic recording (HAMR), a tiny area of the magnetic media has to be heated up to a somewhat high temperature (> 400 °C) [30], typically with laser, to lower the coercivity and immediately followed by applying a writing field to record information on the area. During heat applying, it is estimated that laser induced heating rates in HAMR are in the of order 10^{11} to 10^{12} K/s (depending on the laser power) and the laser heating duration in one heating and cooling cycle in HAMR could be as short as 1 ns [31]. Hence, temperature raised in real HAMR application could to up 1000 K. Therefore, to comply with the estimated temperature in real application, in this work, the heat applying duration t_0 is ranging from 0 to 2 ns for the laser power ranging from 8 to 12 mW so that the increase in temperature could be scaled with that in real application and cover the critical temperature of bulk FePt.

On the investigation of effect the heat source power and the duration of heating time, Fig. 3a shows the minimum normalized magnetization value ($m_{\min}$) associated to sets of heating condition (P, t_0) in the 3 layered films. As can be seen, smaller $m_{\min}$ can be obtained with increasing t_0 or P as more thermal energy is provided into the system. However, at low P the reduction in $m_{\min}$ with increasing t_0 is not significant above a critical time, e.g. $t_0 > 0.8$ ns for $P = 4$ mW, as steady state temperature is low and easily reached even at low t_0 (i.e. T does not change with time in Fig. 1a). Further, to summarize the heating effect on $m_{\min}$ value, Fig. 3b shows $m_{\min}$ values as a function of t_0 for

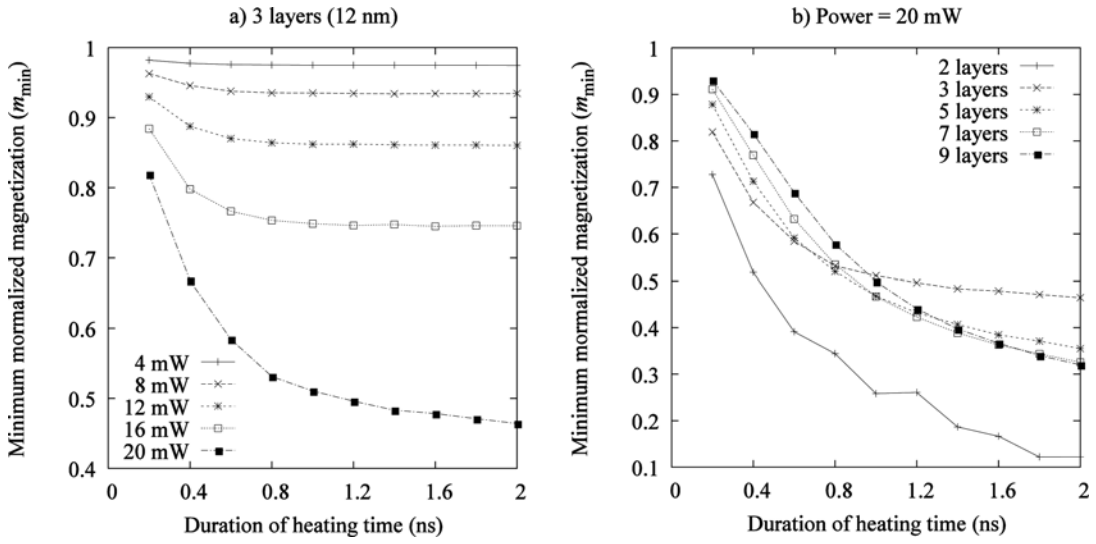

Fig. 3. The minimum normalized magnetization $m_{\min}$ as a function of duration of heating time t_0 simulated using (a) $P = 4$ mW to 20 mW for 3 layered films, and (b) $P = 20$ mW but varying films thickness from 2 to 9 layers.

films with thickness l ranging from 2 to 9 layers simulated at P = 20 mW. As can be seen, very complex behavior is found. For instance, at low t_0, m_{min} is larger with increasing the films thickness. This is as the average ferromagnetic interaction is stronger in thicker films (due to the cease in surface effect) so the ferromagnetic order and m_{min} are stronger. Nevertheless, at larger t_0, m_{min} of the 2 layered films continues to drop but that of the 3 layered changes its trend to a very slow drop which results largest m_{min} at t_0 = 2.0 ns. Notice that, for $l > 2$, $m_{min}(l = 3) < ... < m_{min}(l = 9)$ at small t_0, but $m_{min}(l = 3) > ... > m_{min}(l = 9)$ at large t_0 (e.g. t_0 = 2.0 ns).

To describe the complex behavior in Fig. 3b, the surface temperature profile of the films at P = 20 mW was considered. Figure 4a presents the results for small t_0 = 0.4 ns and Fig. 4b presents the results for large t_0 = 2.0 ns. In Fig. 4a, at t_0 = 0.4 ns, it is found $T_{max}(l = 2) < T_{max}(l = 3) < T_{max}(l > 3)$, where $T_{max}(l > 3)$ are not very much different and $T_{max}(l = 2)$ almost reaches the stead state. However, it is well-known that the critical temperature T_C in films system reduces with reducing the films thickness, where the thickness dependent critical temperature $T_C(l)$ can be estimated by the equation [2].

$$\frac{1}{T_C(l)} = \frac{1}{4.539}\left[1 + \left(\frac{1.01}{l + 0.01}\right)^{1.280}\right], \quad (16)$$

with numerical values presented in Table 1.

Therefore, even $T_{max}(l = 2)$ on the topmost surface is the smallest but with its value just above the 2 layered critical point, the smallest m_{min} is found. Note that, the layers below the topmost may have lower temperatures but in the 2 layered case the films is very thin allowing large influence from thermal fluctuation. Therefore, smallest m_{min} value is appropriate. The same reason also applies for of all considered films, but it is found that $m_{min}(l = 2) < ... < m_{min}(l = 9)$. This is as the thicker the films the more number of layers having smaller temperatures than that of the topmost surface. Further, these underneath layers may have temperatures smaller than the critical point, so the ferromagnetic ordering is stronger in thicker films resulting in larger m_{min}.

Table 1. Ising critical temperatures for simple cubic films.

Number of layers (l)	Critical point (T_C, J/k_B)	Critical point (T_C, K)
2	3.212	533.98
3	3.641	605.44
5	4.023	668.79
7	4.189	696.48
9	4.280	711.56

On the other hand, in Fig. 4b at where t_0 = 2.0 ns, it is found that $T_{max}(l = 2) < ... < T_{max}(l = 9)$, and the time for reaching the steady state increases. As a result, the 2 layered films, with lower critical point T_C than the steady state temperature in Fig. 4b, m_{min} continuously drops to its paramagnetic value (m_{min} = 0). However, the 3 layered films have T_C higher than that of the 2 layered films, where this T_C may be larger than the overall steady state temperature of the 3 layered films (averaged from all 3 layers). Therefore, in Fig. 3b, $m_{min}(l = 3)$ is somewhat high. On the

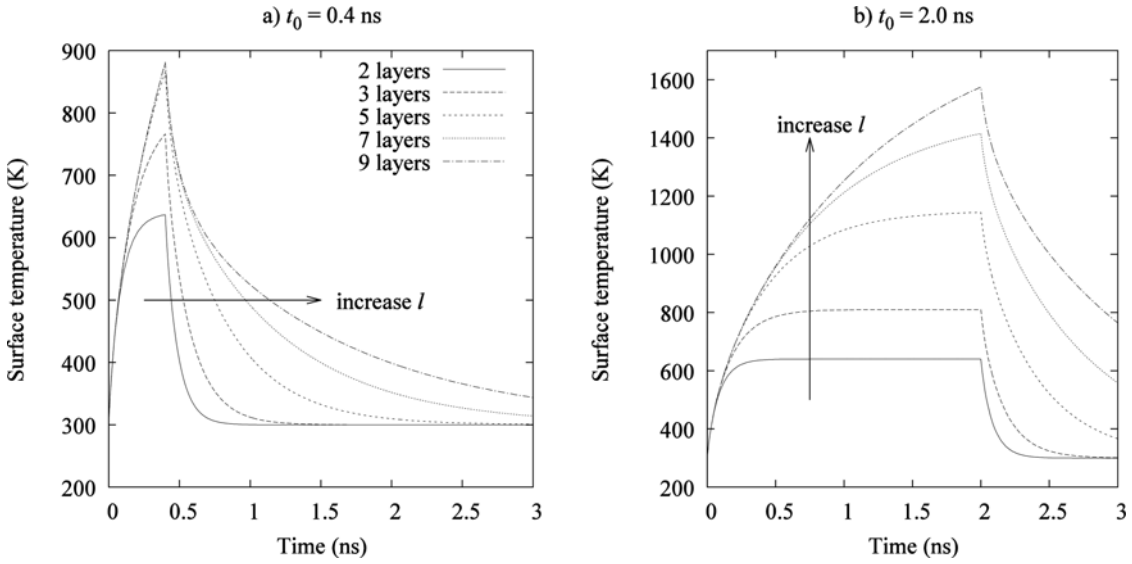

Fig. 4. The topmost surface temperature of films simulated using the heat source P = 20 mW and the duration of heating time (a) t_0 = 0.4 ns and (b) t_0 = 2.0 ns as a function of observed time with varying films thickness l. Key to the symbols in (b) is the same as that in (a).

other hand, for $l > 3$, the critical temperature T_C increases for thicker films but the increasing step is not as much as from 2 to 3 layers, e.g. see Table 1. Nevertheless, though with the higher temperature allowed for thicker films ($l > 3$) at $t_0 = 2.0$ ns in Fig. 4b, the overall averaged temperature from all layer drops with increasing films thickness. Consequently, that $m_{\min}(l = 3) > ... > m_{\min}(l = 9)$ at $t_0 = 2.0$ ns becomes sensible in Fig. 3b. Examples of how temperatures decrease with distance away the hot boundary can be found in Ref. [6].

As one can see, the heat transferring effect on ferromagnetic stability magnitude, i.e. the magnetization m, is rather complicated especially when the films thickness is taken into account. This is as the parameters, which are heat source power (P), the heating duration (t_0), the films thickness (l), the steady state temperature and the films critical point (T_C), are all related and have a strong effect on the ferromagnetic order. However, based on the findings in this work, one may see some benefit on using the database proposed in the work (e.g. Figs. 1 to 4) as a guideline for designing more efficient heat assisting magnetic applications.

Note that apart from laser heating method, it is also possible to apply the Joule heating technique to heat the magnetic media up to desired temperatures [32]-[35]. The idea is lying on current induced either magnetic domain wall motion or magnetization switching. With this current induced heat procedure, it may be possible to overcome the laser-wavelength focusing problem when the magnetic grain size is very small. These therefore open window of opportunities to tackle the energy assisted magnetic recording problem from the current heating side rather than the laser heating technique.

6. Conclusion

In this work, Monte Carlo simulation was used to investigate time-dependent magnetization behavior of ferromagnetic films consisting of several nano-magnetic grains in thickness, under the effect of supplied heat pulse on the films surface. The Ising model and Metropolis algorithm were used to update magnetic spins in extracting the magnetization, while the finite difference technique was used to calculate spatial- and time-dependent temperatures. Using the parameters from FePt as an application, the time-dependent magnetization profiles for various heat source power, heat applying duration (time), and films thickness were investigated where appropriate magnetization behavior related to relevant parameters were proposed.

References

[1] T. Osaka, T. Asahi, J. Kawaji, and T. Yokoshima, Electrochim. Acta **50**, 4576 (2005).
[2] Y. Laosiritaworn, J. Poulter, and J. B. Staunton, Phys. Rev. B **70**, 104413 (2004).
[3] J.-S. Suen, M. H. Lee, G. Teeter, and J. L. Erskine, Phys. Rev. B **59**, 4249 (1999).
[4] Y. Li, J.-H. Moon, and K.-J. Lee, J. Magnetics **16**, 323 (2011).
[5] J. Eisenmenger and I. K. Schuller, Nature Mater. **2**, 437 (2003).
[6] Y. Laosiritaworn, S. Ananta, and R. Yimnirun, Phys. Rev. B **75**, 054417 (2007).
[7] M. E. J. Newman and G. T. Barkema, Monte Carlo Methods in Statistical Physics, Clarendon Press, Oxford (1999).
[8] O. A. Ivanov, L. V. Solina, V. A. Demshima, and L. M. Maget, Phys. Met. Metall. **35**, 81 (1973).
[9] D. Weller, A. Moser, L. Folks, M. E. Best, W. Lee, M. F. Toney, M. Schwickert, J.-U. Thiele, and M. F. Doerner, IEEE Trans. Magn. **36**, 10 (1987).
[10] Y. K. Takahashi, T. Koyama, M. Ohnuma, T. Ohkubo, and K. Hono, J. Appl. Phys. **95**, 2690 (2004).
[11] B. Xu, C. W. Chia, Q. Zhang, Y. T. Toh, C. An, and G. Vienne, Jpn. J. Appl. Phys. **50**, 09MA05 (2011).
[12] J. B. Staunton, L. Szunyogh, A. Buruzs, B. L. Gyorffy, S. Ostanin, and L. Udvardi, Phys. Rev. B **74**, 144411 (2006).
[13] J.-U. Thiele, K. R. Coffey, M. F. Toney, J. A. Hedstrom, and A. J. Kellock, J. Appl. Phys. **91**, 6595 (2002).
[14] Z. Li, D. Wei, and F. Wei, J. Magn. Magn. Mater. **320**, 3108 (2008).
[15] O. Hovorka, S. Devos, Q. Coopman, W. J. Fan, C. J. Aas, R. F. L. Evans, Xi Chen, G. Ju, and R. W. Chantrell, Appl. Phys. Lett. **101**, 052406 (2012).
[16] S. Greaves, Y. Kanai, and H. Muraoka, IEEE Trans. Magn. **48**, 1794 (2012).
[17] P.-W. Huang, X. Chen, and R. H. Vitora, IEEE Trans. Magn. **48**, 3188 (2012).
[18] T. W. McDaniel, J. Appl. Phys. **112**, 013914 (2012).
[19] I. Hatta, Thermochim. Acta **446**, 176 (2006).
[20] Y. K. Takahashi, T. Koyama, M. Ohnuma, T. Ohkubo, and K. Hono, J. Appl. Phys. **95**, 2690 (2004).
[21] B. Xu, H. Yuan, J. Zhang, R. Ji, Q. Zhang, X. Miao, and T. C. Chong, J. Magn. Magn. Mater. **320**, 731 (2008).
[22] N. Metropolis, A. W. Rosenbluth, M. N. Rosenbluth, A. H. Teller, and E. Teller, J. Chem. Phys. **21**, 1087 (1953).
[23] Y. Laosiritaworn, Thin Solid Films **517**, 5189 (2009).
[24] Y. Laosiritaworn, IEEE Trans. Magn. **45**, 2659 (2009).
[25] Y. Laosiritaworn, Adv. Mater. Res. **55**, 385 (2008).
[26] L. Néel, Adv. Phys. **4**, 191 (1955).
[27] W. F. Brown Jr., IEEE Trans. Magn. **15**, 1196 (1979).
[28] A. M. Ferrenberg and D. P. Landau, Phys. Rev. B **44**, 5081 (1991).

[29] J.-U. Thiele, K. R. Coffey, M. F. Toney, J. A. Hedstrom, and A. J. Kellock, J. Appl. Phys. **91**, 6595 (2002).
[30] Y. Ma, X. Chen, and B. Liu, Microsyst. Technol. *In press* DOI 10.1007/s00542-012-1668-9 (2012).
[31] M. H. Kryder, E. C. Gage, T. W. McDaniel, W. A. Challener, R. E. Rottmayer, G. Ju, Y.-T. Hsia, and M. F. Erden, Proc. IEEE **96**, 1810 (2008).
[32] S.-S. Ha, K.-J. Lee, and C.-Y. You, Curr. Appl. Phys. **10**, 659 (2010).
[33] C.-Y. You, S.-S. Ha, and H.-W. Lee, J. Magn. Magn. Mater. **321**, 3589 (2009).
[34] C.-Y. You, I. M. Sung, and B.-K. Joe, Appl. Phys. Lett. **89**, 222513 (2006).
[35] C.-Y. You and S.-S. Ha, Appl. Phys. Lett. **91**, 022507 (2007).